Catal Lett (2007) 118:231–237
DOI 10.1007/s10562-007-9175-9

Low Temperature Preparation and Characterization of N-doped and N-S-codoped TiO_2 by Sol–gel Route

Yi Xie · Qingnan Zhao · Xiu Jian Zhao · Yuanzhi Li

Received: 5 April 2007 / Accepted: 18 June 2007 / Published online: 14 July 2007

Abstract This paper reports a new method to prepare the N-doped and N-S-codoped anatase TiO_2 photocatalysts at 100 °C. The as-prepared photocatalysts were characterized by means of XRD, Raman spectra, TEM, BET, UV–Vis diffuse reflectance spectra (DRS) and XPS. The results showed that the N-doping and N-S-codoping extended the absorbance spectra of TiO_2 into visible region with different extent. The BET surface area of the N-S-codoped TiO_2 photocatalysts was high up to 245 m^2g^{-1}. The results of degradation of methyl orange (MO) solution showed that the N-doped and N-S-codoped TiO_2 photocatalysts exhibited higher photocatalytic activity than that of Degussa P-25 and the as-prepared pure TiO_2 under visible irradiation. This property can be attributed to the results of synergetic effects of absorption in the visible light region, red shift in adsorption edge, good crystallization and large surface area of the as-prepared N-doped or N-S-codoped TiO_2.

Y. Xie · Q. Zhao · X. J. Zhao (✉) · Y. Li
Key Laboratory of Silicate Materials Science and Engineering, Wuhan University of Technology, Ministry of Education, Wuhan 430070 Hubei, P.R. China
e-mail: opluse@whut.edu.cn

Y. Xie
e-mail: xieyithanks@163.com

Q. Zhao
Material Testing Center of Wuhan, University of Technology, Wuhan 430070 Hubei, P.R. China

Keywords Low temperature preparation · Sol–gel · N-S-codoped TiO_2 · Photocatalyst · Visible light

1 Introduction

In the past decades, TiO_2 has been the most widely used and investigated photocatalyst because of its nontoxicity, inexpensiveness, chemical stability and favorable optoelectronic properties. However, it can only work under ultraviolet (UV) light (wavelength $\lambda < 388$ nm) duo to its wide bandgap of 3.0–3.2 eV, which means only about 4% of the incoming solar energy on the surface can be utilized. Many attempts have been made to improve the optical response of TiO_2 under visible light excitation. In recent years, nonmetal doping of TiO_2 rekindled a great interest in visible light catalysis since the report of the work of Asahi et al in 2001 [1]. After that, both the preparation methods and the theoretical calculations have been performed and reported for nonmetal doping of TiO_2 [2–13].

S or N-doped TiO_2 has been prepared by sputtering [1, 8], chemical vapor deposition [9], sol–gel [4, 10–11], ion implantation [12–13] and spray pyrolysis [14]. However, these experiments were performed at high temperatures, which usually led to the grain growth and lowering of the surface area and thus hampered the enhancement of photocatalytic activity. Here we proposed a novel approach to prepare N-doped and N-S-codoped TiO_2 photocatalysts at 100 °C, using tetrachloride titanium as the titanium source and thiourea as nitrogen and sulfur source. The obtained N-doped and N-S-doped titania had high specific surface area, and exhibited higher photocatalytic activity than that of P25 under visible irradiation.

2 Experimental

2.1 Photocatalyst Preparation

$TiCl_4$(Sinopharm Chemical Reagent Co., Ltd, China), distilled water, diluted ammonia (1: 9), H_2O_2 (30%) and thiourea (Shanghai Shiyi Chemicals Reagent Co., Ltd. China) were used for the synthesis of N-doped and N-S-codoped TiO_2. The starting material thiourea was used to introduce nitrogen and sulfur. N-doped and N-S-codoped TiO_2 photocatalysts were synthesized by sol–gel method. The schematic procedure is illustrated in Fig. 1. In a typical preparation, 18 mL of $TiCl_4$ was added dropwise into 1,500 mL distilled water in an ice-water bath with strong magnetic stirring. After stirring for 30 min, the pH of this acidic solution was adjusted to 7 by dropwise addition of diluted ammonia solution. After stirring at this pH for 24 h, the obtained precipitate was filtered and washed thoroughly with distilled water until Cl^- was not detected.. Then, the precepitate was ultrasonic dispersed in 1300 mL distilled water. H_2O_2 (135 mL) was added dropwise into this mixture under stirring. The resulting yellow transparent solution was divided into six portions. A certain amount of thiourea dissolved in 10 ml of absolute ethanol was added to the above solutions. And then, the mixtures were heated at 100 °C for 10 h in a temperature controlled oil bath equipped with a magnetic stirrer, thermometer and reflux condenser. Finally, the resulted precipitates were dried at 80 °C for 24 h and grinned in agate mortar to obtain the powder samples. To prepare N-S-codoped titania with different composition of N and S, the dosage of thiourea was changed. Pure TiO_2 was prepared by a similar procedure without the addition of thiourea.

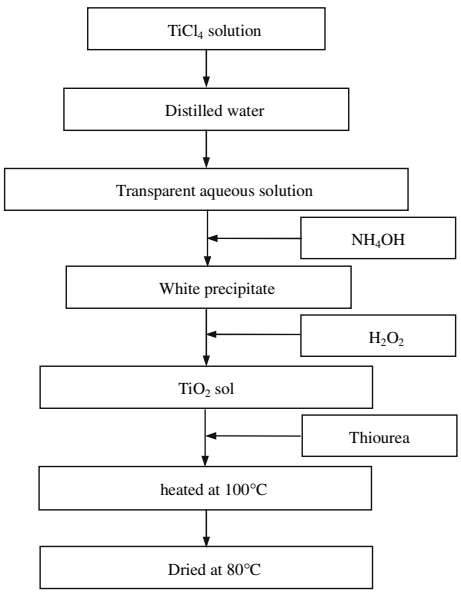

Fig. 1 Process diagram for sol–gel synthesis of N-doped and N-S-codoped TiO_2 powder

2.2 Photocatalyst Characterization

The crystalline structure was identified by X-ray diffraction (XRD) (D/MAX-IIIA, Rigaku, Japan) measurements using Cu Kα (λ = 0.15418 nm) radiation at 35 kV, 30 mA in the 20–80 °C 2θ angle range. The average crystallite size was determined according to the well-known Scherrer equation using the FWHM data after correcting the instrumental broadening [15]. The crystalline structure was also investigated by Raman spectroscopic measurements (InVia, Renishaw, Britain), performing at room temperature in air using the 514.5 nm line of argon gas laser as excitation.

Transmission electron microscopy (TEM) measurements were carried out with a JEM-2010 (Japan) microscope operating at 200 kV in the mode of bright field.

Brunauer–Emmett–Teller (BET) surface area (S_{BET}) of the powders was analyzed by nitrogen adsorption in an AUTOSORB-1 (Quantachrome Instruments, USA) nitrogen adsorption apparatus. All the samples were degassed at 100 °C prior to actual measurements. The S_{BET} was determined by a multipoint BET method using the adsorption data in the relative pressure (P/P_0) range of 0.05–0.25.

UV–Vis diffuse reflectance spectra (DRS) of the photocatalysts were measured on a UV-2550 (Rigaku, Japan) instrument equipped with integrating sphere accessory with the wavelength ranging from 300 to 600 nm. $BaSO_4$ was used as the standard for these measurements.

X-ray photoelectron spectroscopy (XPS) measurements were performed on an ESCALAB MK II spectrometer (VG Scientific Ltd. UK.) with non-monochromatic Al Kα X-ray (1486.6 eV). The pressure in the chamber during the experiments was about 10^{-7}Pa. The analyzer was operated at 50 eV pass energy for high resolution spectra and 100 eV for survey spectra. The binding energy of the C1s line (284.6 eV) was taken for calibrating the obtained spectra. Background subtraction and peak fitting was performed using a public XPS peak fit program (XPSPEAK4.1 by R. Kwok). Recorded spectra were fitted using Gauss–Lorentz curves and the Lorenz–Gauss ratio for each Ti, O, S and N species was kept constant.

2.3 Evaluation of Photocatalytic Activity

Photocatalytic activity of the as-prepared samples and Degussa P-25 was evaluated by the degradation of methyl orange (MO), which was performed in a 100 mL beaker reactor. For each condition, 160 mg of powders was added into 40 mL of aqueous solution of MO (10 mg L^{-1}). The catalysts were stirred for 15 min in the dark to get the

equilibrium of MO adsorption-desorption followed by switching on light. Photodegradation of MO was performed at room temperature by using a high pressure Hg-light (125 W) with the UV cut-off filter. The UV cut-off filter was placed between the beaker and light source to exclude ultraviolet radiation under 420 nm. The incident intensity to the sample surface was 254 μ W cm $^{-2}$. The photocatalytic experiment was repeated under the identical reaction conditions to confirm the reproducibility. At the given intervals, a few milliliter of the mixtures were drawn from the beaker, and filtered by centrifugation. Its UV–Vis spectra were recorded on a UV–Vis spectrophotometer (UV-1601, Rigaku, Japan). The relative concentration of MO was monitored by comparing its absorbance at 464 nm with that of the original solution [16].

3 Results and Discussion

3.1 Characterization of N-doped and N-S-codoped TiO_2

The powder XRD patterns of the synthesized N-doped and N-S-codoped TiO_2 samples are shown in Fig. 2. The diffraction peaks at $2\theta = 25.14°$, 37.75°, 47.95°, 54.13°, 62.72° corresponding to the anatase phase of titania (PDF: 21–1272) are observed in all the samples heated at 100 °C for 10 h. Usually, the amorphous-anatase transformation may complete in the temperature range from 250 to 400 °C, while anatase TiO_2 with a small amount of brookite has been prepared even at 40 °C [17]. The peak positions are nearly the same and no extra peaks except for anatase $TiO_2$are observed, suggesting that the structure of TiO_2 is not changed. The intensity of (101) peak increases initially with increasing molar ratio of thiourea/TiO_2 and decreases when the ratio was higher than 20/100. This observation suggests that the addition of thiourea might enhance the formation and growth of TiO_2 anatase phase, but the surplus thiourea might be unfavorable for the formation of anatase. Compared to pure TiO_2, the codoped photocatalysts show a slight shift of the (101) peak, indicating a lattice distortion of the doped photocatalysts [4]. The average crystallite sizes of the samples are calculated using the Debye–Scherrer equation, and given in Table 1 together with other physical properties. The crystallite sizes of samples are in the range of 5–8 nm, which is promising since nanocrystalline anatase has being considered as the more photoactive form of TiO_2.

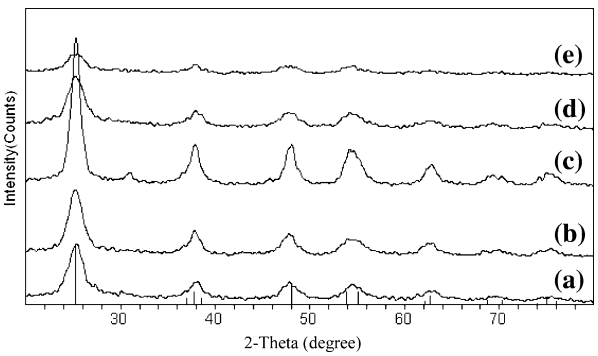

Fig. 2 X-ray diffraction patterns of N-doped and N-S-codoped TiO_2 prepared from precursors with different molar ratio of thiourea/Ti: (**a**) 3/100; (**b**) 5/100; (**c**) 20/100; (**d**) 40/100; (**e**) 100/100 and compared to the JCPD file (bottom plot) of anatase TiO_2 (PDF: 21–1272)

Raman spectra of the selected N-doped and N-S-codoped TiO_2 photocatalysts are shown in Fig. 3. There is a sharp Raman peak at about 150 cm^{-1} and three weak peaks at about 400, 516 and 640 cm^{-1}, which can be attributed to the Raman-active modes of anatase phase with the symmetries of E_g, B_{1g}, A_{1g} or B_{1g}, and E_g, respectively [18].

The structure of N-S-codoped TiO_2 was further studied by TEM image and selective area electron diffraction (SAED) (inset, Fig. 4). It can be seen that N-S-codoped TiO_2 crystals have rodlike morphology. SAED analysis further confirmed that TNS3 has anatase structure. The results of Raman and SAED are in fully agreement with that of XRD (Fig. 2).

Figure 5 shows the nitrogen adsorption/desorption isotherms for the as-prepared samples. All the isotherms are type IV, which is the characteristic of mesoporous materials [19–20]. Their specific surface area (S_{BET}) are shown in Table 1. All the samples show high surface area in the range of 213–245 m^2 g^{-1}, which is much higher than those of most nonmetal-doped TiO_2 reported in the literatures [3, 10, 21]. It can be concluded that the present wet chemical process is a good route for preparation of porous photocatalysts with high surface areas, which is favorable in enhancing the photocatalytic activity of TiO_2-based photocatalysts.

Figure 6 displays the UV–Vis DRS of the as-prepared samples with different molar ratios of thiourea to TiO_2. The pure TiO_2 only exhibit a absorption band in the UV region, whereas the doping of nitrogen and sulfur extended the absorbance from UV to visible region. The absorption edge shifts from 387 to 510 nm with decreasing initial molar ratio of thiourea/TiO_2 from 100/100 to 3/100. The absorption intensity of the samples in the visible region decreases with increasing initial thiourea content. As reported, nonmetal-doped TiO_2 is generally yellow [10, 24,]. Here, we observed that the yellow color of the as-prepared photocatalysts became paler with increasing thiourea content in the starting materials (Table 1).

As shown in Fig. 7, both of the XPS survey scans of the as-prepared TN2 and TNS3 show predominantly oxygen, titanium, nitrogen and carbon. A signal of S 1s is also detected for sample TNS3. Carbon could be originated

Table 1 Characterization results for N-doped and N-S-codoped TiO_2photocatalysts

Sample	Molar ratio of thioure/TiO_2	Color of catalyst	SBET (m^2 g^{-1})	DScherrer (nm)	Decomposition of methyl orange after 24 h irradiation (%)
TN1	3/100	Yellow		5	38.3
TN2	5/100	Yellow	241	5	95.5
TNS3	20/100	Light yellow	245	8	96.6
TNS4	40/100	Light yellow	213	5	89.3
TNS5	100/100	White yellow		5	55.5
TiO2		Yellow			35.3
P25		White			70.9

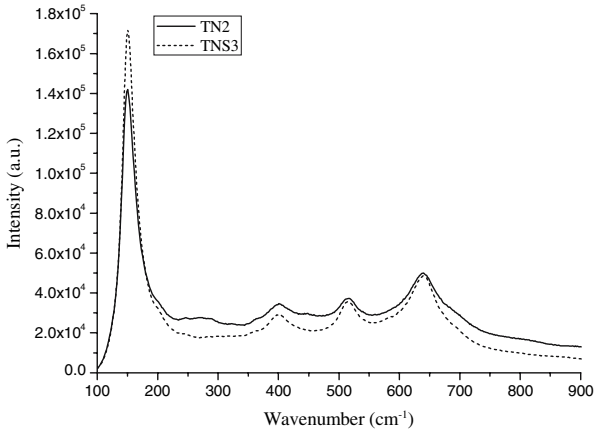

Fig. 3 Raman spectra of N-doped (TN2) and N-S-codoped (TNS3) TiO_2 photocatalysts

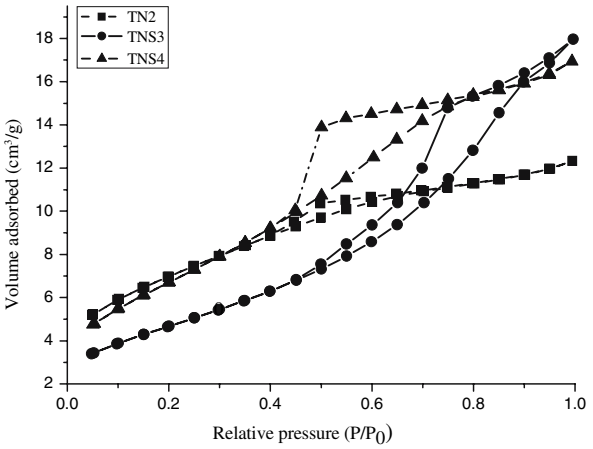

Fig. 5 N_2 adsorption-desorption isotherms of the as-prepared samples

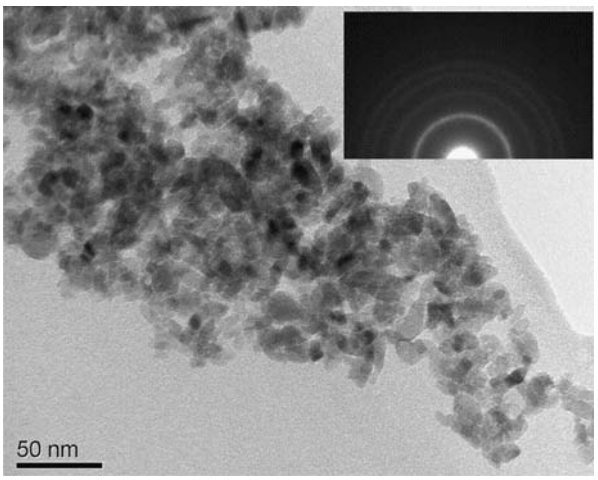

Fig. 4 A representative TEM image and selected area electron diffraction (SAED) pattern of the as-prepared sample TNS3

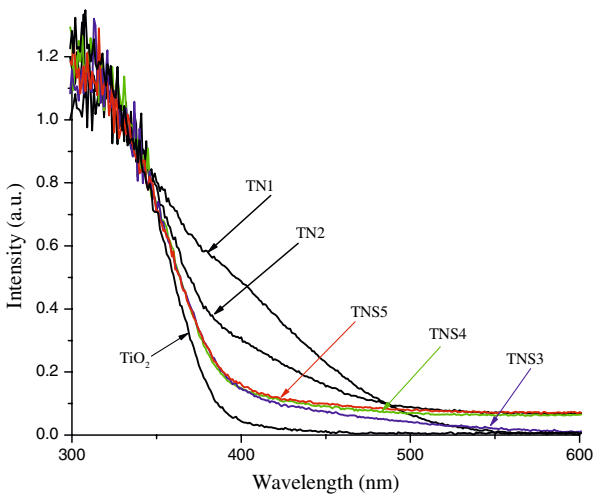

Fig. 6 UV–Vis diffuse reflectance spectra of N-doped and N-S-codoped TiO_2 prepared from precursors with different molar ratio of thiourea to TiO_2

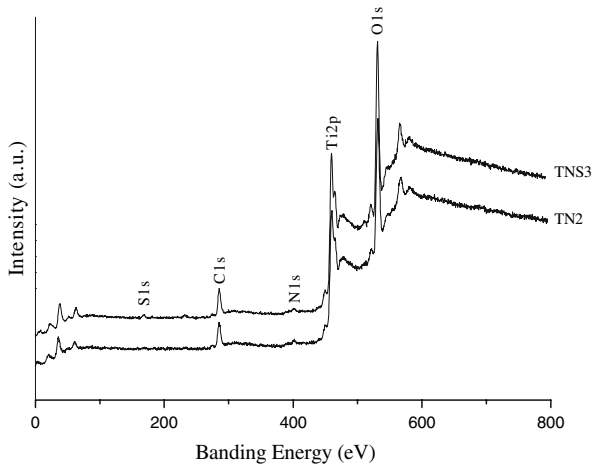

Fig. 7 Survey scans results of the XPS spectra of N-doped (TN2) and N-S-codoped (TNS3) TiO_2 photocatalysts

from adventitious carbon due to exposure to ambient pressure during the preparation.

High-resolution XPS spectra of Ti 2p, O 1s, N 1s and S 2p lines were measured for the samples TN2 and TNS3 (Fig. 8). The results by curve fitting were shown in Table 2. As indicated in Table 2, oxygen is deficient in a stoichiometric ratio. The total N content in sample TN2 is 3.90 at.%, higher than that in sample TNS3 (at. 2.24%). The amount of S in sample TNS3 is estimated to be 2.18 at.%.

XPS spectra of Ti 2p showed a doublet peaks at 458.2 (459.0) and 463.9 (464.7) eV for Ti $2p_{3/2}$ and Ti $2p_{1/2}$ lines (Fig. 8a), respectively, which are assigned to the Ti^{4+} oxidation state according to the reported XPS data [22–23]. The O 1s core level spectra are asymmetric (Fig. 8b). By curve fitting, the peak of O 1s at 530.0 (530.1) eV corresponds to lattice oxygen of TiO_2, and a shoulder peak at higher binding energy of 531.7 (531.9) eV is assigned to mixed contributions from surface hydroxides.

Many researchers reported that sulfur and nitrogen doping induce visible light absorption and response [24–30]. To investigate the states of sulfer and nitrogen, the S 1s and N 1s core levels were also measured by XPS. In contrast to the studies using thiourea as S sources [4, 24], both peaks attributed to N and S atoms were detected in our samples when the molar ratio of thiourea/TiO_2 was higher than 20/100, and only N atom was detected for sample TN2 (Fig. 8c,d). The latter was resulted from the loss of S during heating at 100 °C. The oxidation state of the S-dopant is dependent on the preparation methods, and it was reported that anionic sulfur doping is difficult to carry out because S^{2-}(1.7 Å) has a much larger ionic radius compared to that of O^{2-} (1.22 Å) [6]. Ohno et al. also obtained cationic S-doped TiO_2 [24–25]. As shown in Fig. 8c, the S 2p XPS spectrum centered at 167.8 eV is similar to S^{4+} species that observed in Refs.[24, 26–27] The incorporation of S^{4+} species into TiO_2 was reported to locally distort the lattice of TiO_2 powders [24]. Figure 8d displays N 1s

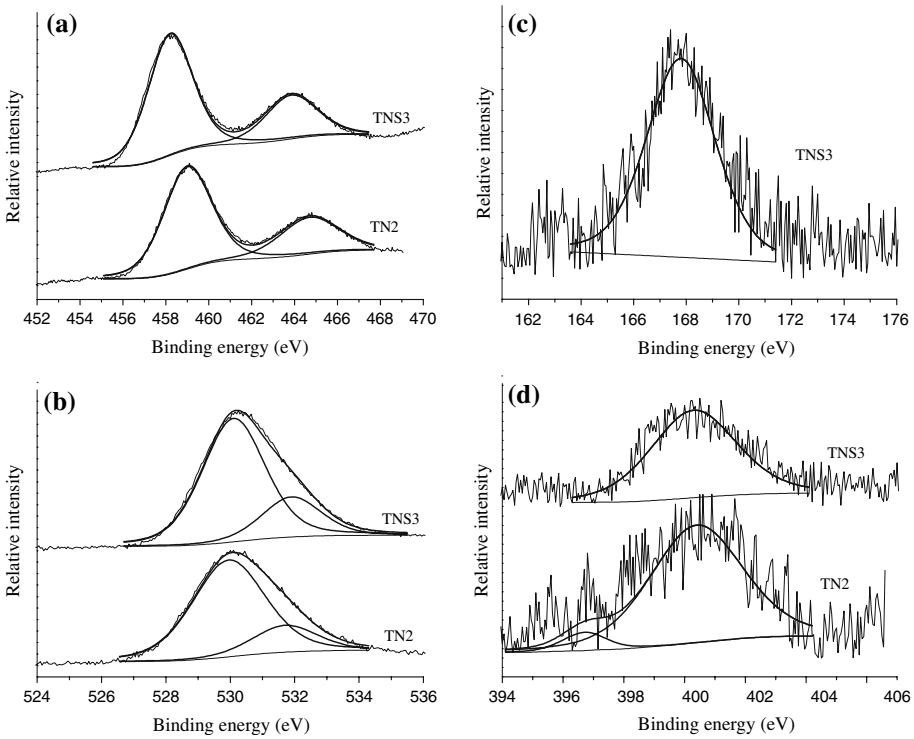

Fig. 8 High-resolution XPS spectra of Ti 2p (**a**), O 1s (**b**), S 2p (**c**), and N 1s (**d**) of the as-prepared N-doped (TN2) and N-S-codoped TiO_2 (TNS3)

Table 2 Binding energies and relative contents of the Ti 2p, O 1s, S 1s and N 1s

Sample		Ti		O		S	N	
		Ti ($2p_{3/2}$)	Ti ($2p_{1/2}$)	Bulk (O^{2-})	OH	SO_x	Ti–N	NO_x
TN2	BE (eV)	459.0	464.7	530.0	531.7		396.7	400.4
	Content (at.%)	27.76		54.73	13.61		0.27	3.63
TNS3	BE (eV)	458.2	463.9	530.1	531.9	167.8		400.3
	Content (at.%)	26.63		52.80	16.15	2.18		2.24

spectra from the surfaces of TN2 and TNS3, respectively. As for the sample TN2, a weak peak centered at 396.7 eV is also detected, which is close to that reported by Nambu et al. [13]. The binding energy around 396 eV were generally considered as the evidence for the presence of Ti–N bonds [1, 9, 21, 28]. Although the amount of this kind of N species is slight (0.27 at.%), it may contribute to the strong absorption of visible light shown in Fig. 6 (TN2). The assignment of N 1s peaks ranging in the 398–403 eV is still under debate. The N 1s XPS peaks at 398.2 eV [3], 400 eV [28] and 401.5 eV [29] were assigned to the formation of N–Ti–O linkages. However, the peaks at 400±0.2 eV [12], 401 eV [30] and 402 eV [31] were assigned to the chemisorbed molecular γ-N state. Additionally, the N 1s core level at 400 eV [7] and 400.2 eV [32] for the N-doped TiO_2 were attributed to NO-like species. The differences discussed above may be due to the differences of preparation procedure. Considering the consistency with the results of the DFT calculations [13], we attribute the N 1s peak at 400.4 eV to the NO_x species as shown in Fig. 8d.

3.2 Visible Light Catalytic Performance

The results of photocatalytic decomposition of MO by different samples are shown in Fig. 9. It can be seen that the N-doped and N-S-codoped TiO_2 samples show much higher photocatalytic activities under visible light ($\lambda \geq 420$ nm) than pure TiO_2. Among them, TNS3 shows the highest photodegradation activity with a MO conversion of 90.6% and 96.6% after 8 and 24 h under visible light irradiation, respectively. In contrast, the pure TiO_2 shows little visible-light-induced photocatalytic activity and the decomposition rate of MO on the P25 TiO_2 is also small. These results indicate that the doping of N or codoping of N and S is an effective way to improve the visible-light-induced photocatalytic activity of TiO_2-based catalysts for the decomposition of organic compounds.

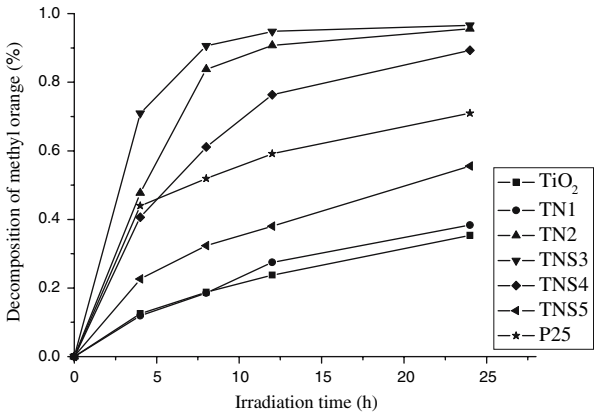

Fig. 9 Effect of ratio of thiourea to TiO_2 on methyl orange decomposition under visible light irradiation

The degradation of MO solution on the prepared pure TiO_2 and commercial P25 TiO_2 could be on the basis of photosensitization process of dyes under visible light irradiation [33]. The photocatalytic activity of TiO_2-based photocatalyst is due to the production of excited electrons in the conduction band and positive holes in the valence band by the absorption of UV or visible illumination. Practically, the photoactivity of a photocatalyst is affected by many factors such as surface area, crystallinity, surface hydroxyl density, and oxygen vacancies [35]. At wavelengths $\lambda \geq 420$ nm, the intensity of absorption spectra are different for all the samples. In addition, the surface area and crystalline size are different, resulting in the different recombination rate of electron–hole pair. Overall, the high visible-light-induced catalytic activity is attributed to the synergetic effects of strong absorption in the visible light region, red shift in adsorption edge, good crystallization and large surface area of the N-doped or N-S-codoped TiO_2. It should be noted that there is not a definite correlation between the light absorption properties and the activity of the samples, that is, the stronger the absorption of visible light does not mean the higher the decomposition rate of MO, typically comparing the corresponding properties of sample TN1 with that of sample TNS3.

4 Conclusions

N-doped and N-S-codoped anatase TiO_2 photocatalysts were prepared at low temperature for the first time. The physical and photocatalytic properties of the photocatalysts prepared with different molar ratio of thiourea to TiO_2 have been compared. Compared with pure TiO_2, UV–Vis DRS

of the N-doped and N-S-codoped TiO_2 photocatalysts showed a shift towards higher wavelengths with absorption edges up to 510 nm. BET surface area was affected by the amount of thiourea. The photocatalysts synthesized with thiourea/TiO_2 ratio of 20/100 had the highest surface area (245 m^2 g^{-1}). The N-doped and N-S-codoped TiO_2 show much higher photocatalytic activity under visible light irradiation than that of pure TiO_2 and Degussa P25 photocatalysts. The process of doping nitrogen or nitrogen and sulfur through wet process at low temperature is promising for preparation of nonmetal-doped TiO_2 with high surface area and high visible-light-induced catalytic activity.

Acknowledgments This research was financial supported by the Program for Changjiang Scholars and Innovative Research Team in University (PCSIRT, No. IRT0547) and the Cultivation Fund of the Key Scientific and Technical Innovation Project (No. 705036), Ministry of Education.

References

1. Asahi R, Morikawa T, Ohwaki T, Aoki K, Taga Y (2001) Science 293:269
2. Khan SUM, Mofareh Al-Shahry, William B (2002) Ingler Jr Sci 297:2243
3. Sathish M, Viswanathan B, Viswanath RP, Gopinath CS (2005) Chem Mater 17:6349
4. Sun HQ, Bai Y, Cheng YP, Jin WQ, Xu NP (2006) Ind Eng Chem Res 45:4971
5. Valentin CD, Pacchioni G, Selloni A (2005) Chem Mater 17:6656
6. Yu JC, Ho W, Yu JG, Yip H, Wong PK, Zhao JC (2005) Environ Sci Technol 39:1175
7. Sato S, Nakamura R, Abe S (2005) Appl Cata A-Gen 284:131
8. Mwabora JM, Lindgren T, Avendano E, Jaramillo TF, Lu J, Lindquist S-E, Granqvist C-G (2004) J Phys Chem B 108:20193
9. Guo Y, Zhang XW, Han GR (2006) Mat Sci Eng B 135:83
10. Bacsa R, Kiwi J, Ohno T, Albers P, Nadtochenko V (2005) J Phys Chem B 109:5994
11. Di Valentin C, Pacchioni G, Selloni A, Livraghi S, Giamello E (2005) J Phys Chem B 109:11414
12. Ghicov A, Macak JM, Tsuchiya H, Kunze J, Haeublein V, Frey L, Schmuki P (2006) Nano Lett 6:1080
13. Nambu A, Graciani J, Rodriguez JA, Wu Q, Fujita E, Fdez Sanz J (2006) J Chem Phys 125:094706
14. Li D, Haneda H, Hishita S, Ohashi N (2005) Mat Sci Eng B 117:67
15. Zhang H, Banfield JF (2000) J Phys Chem B 104:3481
16. Xiao L, Zhang J, Cong Y, Tian B, Chen F, Anpo M (2006) Catal Lett 111:207
17. Li YZ, Lee NH, Hwang DS, Song JS, Lee EG, Kim SJ (2004) Langmuir 20:10838
18. Balachandran U, Eror NG (1982) J Solid State Chem 42:276
19. Yang P, Zhao D, Margolese DI, Chmelka BF, Stucky GD (1999) Chem Mater 11:2813
20. Kruk M, Jaroniec M (2001) Chem Mater 13:3169
21. Yin S, Ihara K, Aita Y, Komatsu M, Sato T (2006) J Photoch Photobio A 179:105
22. Bardi U (1990) Catal Lett 5:81
23. Francisco MSP, Mastelaro VR (2001) J Phys Chem B 105:10515
24. Ohno T, Akiyoshi M, Umebayashi T, Asai K, Mitsui T, Matsumura M (2004) Appl Catal A: General 265:115
25. Ohno T, Mitsui T, Matsumura M (2003) Chem Lett 32:364
26. Rodriguez JA, Liu G, Jirsak T, Hrbek J, Chang Z, Dvorak J, Maiti A (2002) J Am Chem Soc 124:5242
27. Rodriguez JA, Hrbek J, Chang Z, Dvorak J, Jirsak T, Maiti A (2002) Phys Rev B 65:235414
28. Jang JS, Kim HG, Ji SM, Bae SW, Jung JH, Shon BH, Lee JS (2006) J Solid State Chem 179:1067
29. Wang X, Yu JC, Chen Y, Wu L, Fu X (2006) Environ Sci Technol 40:2369
30. Yuan J, Chen MX, Shi JW, Shangguan WF (2006) Int J Hydrogen Energy 31:1326
31. Hong YC, Bang CU, Shin DH, Uhm HS (2005) Chem Phys Lett 413:454
32. Chen H, Nambu A, Wen W, Graciani J, Zhong Z, Hanson JC, Fujita E, Rodriguez JA (2007) J Phys Chem C 111:1366
33. Wu T, Liu G, Zhao J, Hidaka H, Serpone N (1999) J Phys Chem B 103:4862